Journal of Crystal Growth 318 (2011) 846–850

Contents lists available at ScienceDirect

Journal of Crystal Growth

journal homepage: www.elsevier.com/locate/jcrysgro

Recent developments on high Curie temperature PIN–PMN–PT ferroelectric crystals

Shujun Zhang [a,*], Fei Li [a,d], Nevin P. Sherlock [b], Jun Luo [c], Hyeong Jae Lee [a], Ru Xia [a], Richard J. Meyer Jr [b], Wesley Hackenberger [c], Thomas R. Shrout [a]

[a] Materials Research Institute, Pennsylvania State University, University Park, PA 16802, USA
[b] Applied Research Laboratory, Pennsylvania State University, University Park, PA 16802, USA
[c] TRS Technologies Inc., 2820 East College Avenue, State College, PA 16801, USA
[d] Electronic Materials Research Laboratory, Key Laboratory of the Ministry of Education, Xi'an Jiaotong University, Xi'an 710049, P.R. China

ARTICLE INFO

Available online 18 November 2010

Keywords:
A1. Characterization
B2. Ferroelectric materials
B2. Piezoelectric materials

ABSTRACT

$Pb(In_{0.5}Nb_{0.5})O_3$–$Pb(Mg_{1/3}Nb_{2/3})O_3$–$PbTiO_3$ (PIN–PMN–PT) ferroelectric crystals attracted extensive attentions in last couple years, due to their higher usage temperatures range (> 30 °C) and coercive fields (~ 5 kV/cm), meanwhile maintaining similar electromechanical couplings (k_{33} > 90%) and piezoelectric coefficients (d_{33} ~ 1500 pC/N), when compared to their binary counterpart $Pb(Mg_{1/3}Nb_{2/3})O_3$–$PbTiO_3$. In this article, we reviewed recent developments on the PIN–PMN–PT single crystals, including the Bridgman crystal growth, dielectric, electromechanical, piezoelectric and ferroelectric behaviors as functions of temperature and dc bias. Mechanical quality factor Q was studied as a function of orientation and phase. Of particular interest is the dynamic strain, which related to the Q and d_{33}, was found to be improved when compared to the binary system, exhibiting the potential usage of PIN–PMN–PT in high power application. Furthermore, PIN–PMN–PT crystals exhibit improved thickness dependent properties, due to their small domain size, being on the order of 1 μm. Finally, the manganese acceptor dopant in the ternary crystals was investigated and discussed briefly in this paper.

1. Introduction

Relaxor-based $Pb(Mg_{1/3}Nb_{2/3})O_3$–$PbTiO_3$ (PMNT) single crystals offer electromechanical properties that far out-perform polycrystalline PZT based ceramics, making them promising candidates for medical ultrasonic imaging, sonar transducers and solid-state actuators [1–7]. Their relatively low Curie temperatures (T_Cs ~ 130–170 °C), however, limit their applications in transducers, further restricted by ferroelectric phase transitions T_{RM}/T_{MT} (R: rhombohedral; M: monoclinic; T: tetragonal), which occurs at a significantly lower temperature than T_C. Thus, single crystal systems with high T_{RM}/T_{MT} temperatures for enhanced temperature usage range and thermal stability are desired. In addition to the thermal stability requirement, ferroelectric crystals used in electromechanical devices, such as high power sonar transducers, are subjected to high electric fields, where low dielectric/mechanical losses and relatively high coercive fields are necessary. The dielectric loss of PMNT crystals have been reported to be on the order of ≤ 0.4%, similar to the values observed in "hard" PZT based piezoelectrics; however, their mechanical quality factors Q (inverse of mechanical loss of crystals) are found to be ~ 100, similar to "soft" PZT ceramics. Furthermore, the coercive field (E_C) of crystals is on the order of ~ 2 kV/cm, restricting their usage to low ac voltage applications or devices requiring a "biased" drive level.

Recently, numerous researchers have focused on relaxor-PT single crystals with relatively higher T_C and T_{RM}/T_{MT}, including $Pb(Sc_{1/2}Nb_{1/2})O_3$–$PbTiO_3$ (PSNT) and $Pb(Yb_{1/2}Nb_{1/2})O_3$–$PbTiO_3$ (PYNT) [7–9]. The MPB composition in the PYNT system exhibits a T_C of ~ 360 °C, the highest among all the lead based relaxor-PT systems and similar to PZT. Single crystals in the PYNT system were grown using the flux method, with T_C and T_{RT} observed to be ~ 325 and 160 °C, respectively. The increased T_{RT} results in a broadened temperature usage range and improved temperature dependent property [7]. New perovskite single crystals in $(1-x)BiScO_3$–$xPbTiO_3$ (BSPT100x) system were also explored, where a Curie temperature around ~ 400 °C and T_{RT} of 350 °C for BSPT57 single crystals were observed [10–12]. Analogous to PSNT and PYNT systems, however, BSPT crystals have only been grown using the high temperature flux method with limited growth, being on the order of millimeter size. In order to obtain high T_C/T_{RT} large size single crystals, two approaches have been used, including solid state crystal growth (SSCG) of $Pb(Mg_{1/3}Nb_{2/3})O_3$–$Pb(Zr,Ti)O_3$ [13] and modified Bridgman growth of $Pb(In_{0.5}Nb_{0.5})O_3$–$Pb(Mg_{1/3}Nb_{2/3})O_3$–$PbTiO_3$ (PIN–PMN–PT) single crystals [14–27].

In this paper, recent developments on PIN–PMN–PT single crystals are reviewed and compared to PMNT, including the

* Corresponding author. Tel.: +1 814 863 2639; fax: +1 814 865 2326.
E-mail address: soz1@psu.edu (S. Zhang).

0022-0248/$ - see front matter © 2010 Elsevier B.V. All rights reserved.
doi:10.1016/j.jcrysgro.2010.11.043

Bridgman growth method and the dielectric, piezoelectric and ferroelectric behaviors as functions of temperature and dc bias. Mechanical quality factor (inverse of loss) was studied in relation to the engineered domain configuration and/or acceptor modifications, under small signal and dynamic test conditions. Thickness dependent properties of PIN–PMN–PT crystals were also studied for potential high frequency applications.

2. Experimental

Pure and manganese modified PIN–PMN–PT ternary single crystals, with ~75 mm in diameter and >100 mm in length, were grown along the [0 0 1] crystallographic direction by seeded Bridgman technique. The starting compositions were PIN–PMN–PT with 26–36% PIN and 28–32% PT; the manganese modification was in the range of 0.5–5 mol%, above which, the dopant will deteriorate the congruently melting. In Bridgman growth process, cylindrical platinum crucibles charged with PIN–PMN–PT starting materials were placed in a two-zone furnace. The temperature of the upper-zone was set at 80–120 °C higher than the melting point of the ternary compound (~1300 °C), while the lower-zone temperature was 300–500 °C lower, with an axial temperature gradient being on the order of 30–50 °C/cm. After the charge was melted in the upper zone, the crucible was slowly lowered through the temperature gradient to allow unidirectional crystallization [23]; after the growth process, the crystal slowly cooled down to room temperature at 10–30 °C/h to avoid the crystal crack. An as-grown crystal boule, being 75 mm in diameter and 100 mm in length, is shown in Fig. 1 (small inset). Analogous to binary PMNT crystals, the composition along the growth direction varies due to the large segregation of Ti^{4+} (~0.85), also shown in Fig. 1, where the PT content varied from 28% to 35% along the growth direction, with low PT content observed at the bottom part of grown crystal boules, whereas the top portion generally lies in the high PT tetragonal phase region. The PIN and PMN were found to have less segregation, being about ~1.

Samples with different compositions were oriented along the [0 0 1] direction by real-time Laue X-ray, following the IEEE standard [24], then cut/dice to the proper dimension and polished using 12 μ SiC powder. Vacuum sputtered gold was applied to the sample surfaces as electrodes. Samples with rhombohedral and/or monoclinic phase(s) were poled by applying an electric field of 15 kV/cm at room temperature, while tetragonal crystals were poled at the temperature above T_C, with a small dc electric field of 3 kV/cm. Dielectric behavior under external dc bias was measured as a function of temperature, with dc bias varying from 0 to 20 kV/cm and in 1 kV/cm step. A blocking circuit was used to protect the multifrequency *LCR* meter (HP4284A) under high dc bias field, supplied by a Trek609C-6 high-voltage dc amplifier. The resonance f_r and antiresonance f_a frequencies as functions of temperature were obtained using HP 4194A impedance-phase gain analyzer, connected to a computer controlled temperature chamber. The electromechanical coupling factors and mechanical quality factors were calculated according to the IEEE standard. High field polarization measurements as a function of temperature were performed on [0 0 1] oriented plate samples using a modified Sawyer–Tower circuit and a linear variable differential transducer (LVDT) driven by a lock-in amplifier (Stanford Research system, Model SR830), from which the coercive field and internal bias could be determined.

The dynamic material properties were determined under high drive (1–200 Vpk) conditions. A linear frequency modulation pulse was generated by the National Instruments PXI-1033, which swept through the sample resonance frequency under a constant applied voltage. Measuring the voltage and current, the complex impedance spectrum was calculated. The vibration velocity was measured by laser velocimeter. From the data, the maximum dynamic strain was calculated from the maximum vibration velocity and sample length, assuming a cosine distribution of strain. The effective mechanical quality factor was also calculated [25].

3. Results and discussions

3.1. Temperature dependent properties

Fig. 2 presents the dielectric permittivity and dielectric loss as a function of temperature and dc bias for PIN-PMN-PT single crystals. As observed for other ferroelectric crystal systems [14], the Curie temperature was found to shift to lower temperatures when the dc bias was lower than a specific threshold field, above which, the Curie temperature increased with increasing dc bias; meanwhile, the rhombohedral to tetragonal phase transition temperatures were found to decrease linearly with increasing dc bias, stabilizing the tetragonal phase. This is due to the fact that the spontaneous

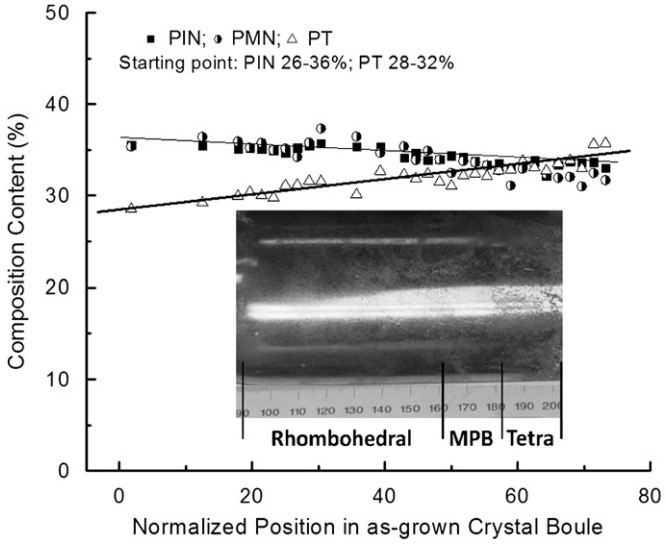

Fig. 1. Compositional variation along the growth direction of as-grown PIN–PMN–PT crystals with 75 mm diameter.

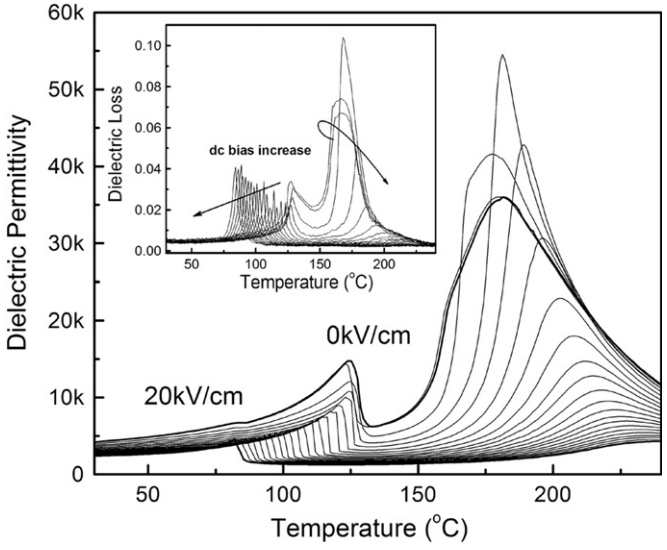

Fig. 2. Dielectric permittivity and dielectric loss (small inset) as function of temperature and external dc bias field for a PIN-PMN-PT with rhombohedral phase.

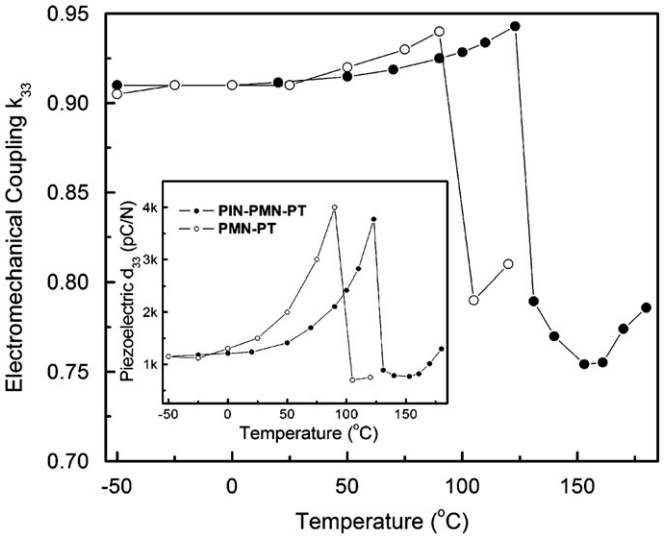

Fig. 3. Electromechanical coupling factor k_{33} and piezoelectric coefficient d_{33} (small inset) as functions of temperature for PIN–PMN–PT and PMNT crystals.

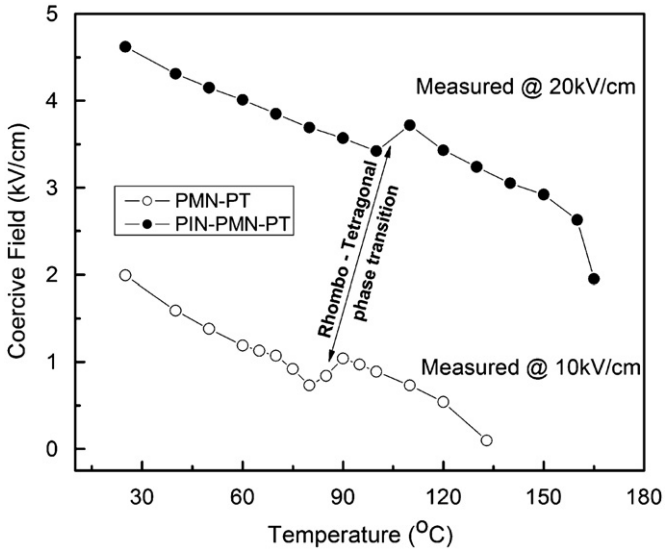

Fig. 4. Coercive field E_C as a function of temperature for PIN–PMN–PT and PMNT crystals.

polarization in tetragonal phase is parallel to the dc bias direction, which was applied along [0 0 1] [21]. Compared to PMNT crystals, the usage temperature range of ternary crystals was found to be ~30 °C higher [21].

Fig. 3 shows the electromechanical coupling k_{33} and piezoelectric coefficient d_{33} (small inset) as functions of temperature for PIN–PMN–PT crystals, compared to PMNT. The electromechanical coupling factors were found to be on the order of 0.90 for both crystals at −50 °C, maintaining similar values with increase in temperature, while the values decrease sharply above ferroelectric phase transition temperatures T_{RT}, due to partial depolarization of the crystals. The piezoelectric coefficients were found to increase with increase in temperature and reach maxima values at the phase transition temperature, whereupon they decreased significantly. Again, as observed in the dielectric behavior, the usage temperature range of PIN–PMN–PT crystal is ~30 °C higher than its binary counterpart.

Fig. 4 gives the coercive field (E_C) as a function of temperature for both PMNT and PIN–PMN–PT crystals. E_C was found to be on the order of 4.6 kV/cm at room temperature for ternary crystals, decreasing to 3.4 kV/cm at 100 °C, due to the easier domain reversal at elevated temperature. The E_C slightly increased to 3.7 kV/cm at 110 °C owing to the coexistence of rhombohedral and tetragonal phases, which was induced by the combination of temperature and electric field, above which the crystals are in tetragonal phase, where the E_C further decreased with increase in temperature. The E_C behavior of PMNT follows similar trend as observed for the ternary crystals, but with much lower values, being on the order of 2 kV/cm at room temperature.

3.2. Mechanical quality factor

To achieve high Q in relaxor-PT crystals, two approaches have been implemented. Fig. 5 presents the mechanical quality factor Q for longitudinal PIN–PMN–PT crystal bars as function of crystallographic orientation and phase. It was found that the Q was maximum for single domain [1 1 1] poled samples, being on the order of ~1000, with values being less than ~200 for [0 0 1] oriented crystals. Of particular significance was the high mechanical Q, being on the order of ~500 for the [1 1 0] engineered domain configuration "2R", with an electromechanical coupling factor k_{33} on the order of ~0.90. The high Q for the domain engineered configuration "2R" ("2R" is one of the domain-engineered structures designated according to the crystal phase and

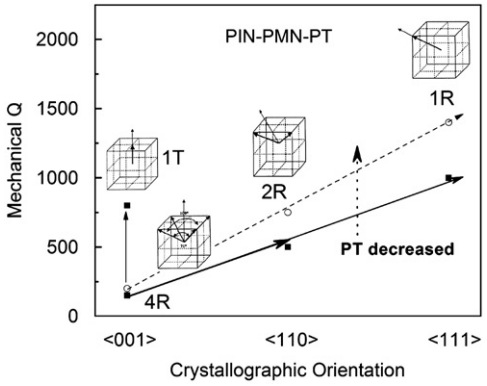

Fig. 5. Mechanical quality factor Q as a function of crystallographic orientations and phase for PIN–PMN–PT crystals (〈0 0 1〉 poled R crystal designated "4R" engineered domain configuration, while 〈1 1 0〉 and 〈1 1 1〉 poled R crystals designated "2R" and "1R", respectively, and 〈0 0 1〉 poled T crystal designated "1T" [28,29]).

poling direction [28,29]) is due to the overall reduced domain wall mobility, while no domain walls exist in single domain state, where much higher Qs are expected [30]. Mechanical Q is not only dependent on the domain configuration, but also on the composition or proximity of the MPB. For lower PT content crystals, being relatively far away from the MPB, higher mechanical Qs were observed. It should be noted that the single domain tetragonal crystals (poled along [0 0 1] direction) possessed Q values, being on the order of > 800. Analogous to "hard" PZT ceramics, acceptor dopants were investigated in PIN–PMN–PT crystals, where the acceptor doping led to the building-up of an internal bias, giving rise to higher Q values due to domain wall pinning/clamping and/or lattice stiffness, revealing that the internal bias contribute to the high Q in doped crystals [31]. Fig. 6 shows the mechanical Q as function of temperature for Mn-doped PIN–PMN–PT crystals along different orientations. The room temperature Q values were found to be on the order of ~800 and 1050 for [0 0 1] and [1 1 0] directions, respectively, decreasing to ~240 and 120 at their ferroelectric phase transition temperatures, above which, Q increased. Correspondingly, the internal bias E_{int} as function of temperature given in the small inset of Fig. 6 showed similar trends as observed for Q values. The faster drop of Q with temperature for [1 1 0] oriented samples is due to rapid decrease of E_{int} with temperature.

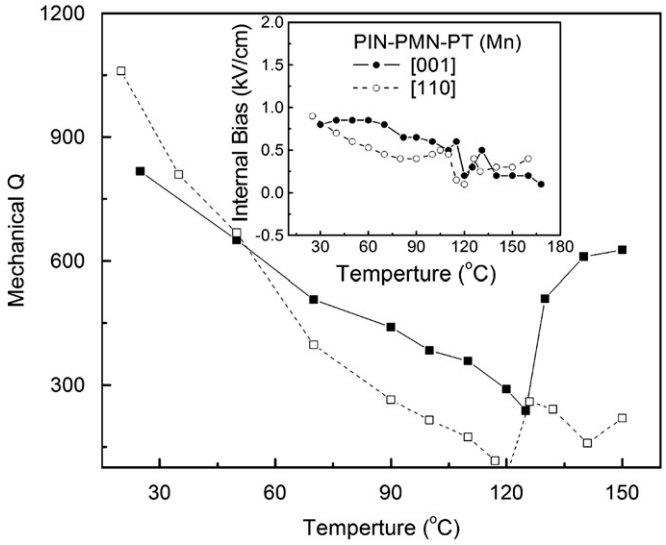

Fig. 6. Mechanical quality factor Q as a function of temperature for Mn-doped PIN–PMN–PT crystals (small inset shows internal bias as a function of temperature).

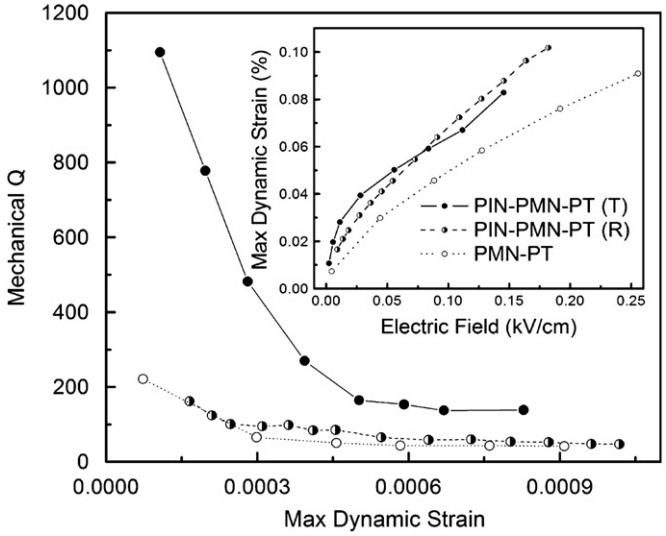

Fig. 7. Mechanical quality factor Q as function of maximum dynamic strain for PIN–PMN–PT with R and T phases, compared to PMNT crystals (small inset shows maximum dynamic strain as fa unction of driving electric field).

The maximum dynamic strains of PIN–PMN–PT and PMNT crystals, measured at resonance frequency, are compared in Fig. 7 (small inset) as a function of peak electric field, where PIN–PMN–PT exhibits greater strain levels than PMNT. Although the small signal $d_{33}Q$ product is often a qualitative indication of dynamic material performance, it is a limited metric for predicting high drive performance [25]. For example, the $d_{33}Q$ product suggests that tetragonal crystals ($>400{,}000$ pC/N) should exhibit greater dynamic strain levels than rhombohedral crystal ($<300{,}000$ pC/N), but Fig. 7 shows the two having similar strain levels. Based on the observed strain, and knowing that Q is a much stronger function of drive level than d_{33}, these data suggest that Q decreases more rapidly for tetragonal crystals as a function of increasing drive. As expected, there is a steep initial drop in Q with increase in dynamic strain (Fig. 7). In the case of tetragonal crystals, however, the drop in Q is proportionally much steeper, with Q values being on the order of $\sim$1000 at low strain level, decreasing to $\sim$140 at a strain level of 0.08%. Meanwhile, the Q values were

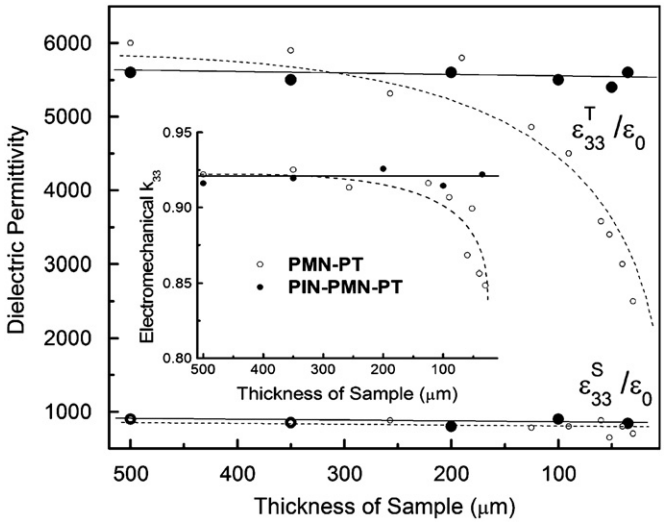

Fig. 8. Dielectric permittivity as a function of sample thickness for PIN–PMN–PT crystals, compared to PMNT (small inset shows coupling factor as a function of sample thickness).

decreased from $\sim$200 to about $\sim$50 with increase in dynamic strain for rhombohedral PIN–PMN–PT and PMNT.

3.3. Thickness dependent properties

It is important to study the thickness dependent properties of relaxor-PT crystals for the high frequency ultrasonic transducer applications, since the frequency range of transducer is closely related to the scale of the piezoelectric element [27,32,33]. From Fig. 8, it was found that the clamped permittivities of both PMNT and PIN–PMN–PT single crystals exhibited similar values across the range of thicknesses; however, the free permittivity of PMNT crystals was strongly affected by the sample scale. At a thickness of $\sim$40 μm, the free permittivity of PMNT crystals was reduced by half. In contrast, PIN–PMN–PT crystals exhibited minimal thickness dependent dielectric properties, even down to thicknesses $\leq$40 μm. As a consequence, the electromechanical coupling factor k_{33} (calculated from the equation $k_{33}=\sqrt{1-(\varepsilon_{33}^{S}/\varepsilon_{33}^{T})}$) of PMNT crystals decreased significantly as a function of sample thickness, while the coupling of PIN–PMN–PT crystals exhibits thickness independent behavior, as shown in the small inset. The underlying mechanism responsible for the degradation in PMNT crystals is believed to be related to their relatively large domains, being on the order of $>$10 μm, where the domains were clamped and polarization rotations suppressed, due to the surface boundary effect when samples scales approach the domain size, while the much smaller domain size of PIN–PMN–PT ($\sim$1 μm) will benefit from the properties at fine scale. More recent research is now carried out on PMNT crystals, in order to get smaller domain size by modified poling condition.

4. Conclusion

In summary, PIN–PMN–PT single crystals with diameters $>$75 mm were grown by the modified Bridgman technique. Piezoelectric and ferroelectric properties were studied as function of temperature, showing a higher usage temperature range for PIN–PMN–PT, when compared to binary PMNT crystals, being on the order of 30 °C. High mechanical quality factor Q was achieved by domain engineering and/or acceptor dopant methods, being 500–800, while maintaining high electromechanical properties. In

addition, PIN–PMN–PT exhibits higher dynamic strain when compared to PMNT, together with its high usage temperature range, high coercive field and small domain size, demonstrating that the ternary crystals are promising candidates for high power and/or high frequency transducer applications.

Acknowledgment

The work was supported by NIH under Grant no. P41-EB21820 and ONR.

References

[1] S.E. Park, T.R. Shrout, IEEE Trans. Ultrason. Ferroelect. Freq. Contr. 44 (1997) 1140–1147.
[2] S.-E. Park, T.R. Shrout, J. Appl. Phys. 82 (1997) 1804–1811.
[3] S. Zhang, L. Lebrun, C. Randall, T. Shrout, J. Cryst. Growth 267 (2004) 204–212.
[4] H.S. Luo, G.S. Xu, H.Q. Xu, P.C. Wang, Z.W. Yin, Jpn. J. Appl. Phys. 39 (2000) 5581–5585.
[5] M. Davis, D. Damjanovic, N. Setter, Phys. Rev. B 73 (2006) 014115.
[6] S.J. Zhang, J. Luo, R. Xia, P.W. Rehrig, C.A. Randall, T.R. Shrout, Solid State Commun. 137 (2006) 16–20.
[7] S.J. Zhang, T.R. Shrout, IEEE Trans. Ultrason. Ferroelectr. Freq. Contr. 57 (2010) 2138–2146.
[8] Y.H. Bing, Z.G. Ye, J. Cryst. Growth 250 (2003) 118–125.
[9] S.J. Zhang, P.W. Rehrig, C.A. Randall, T.R. Shrout, J. Cryst. Growth 234 (2002) 415–420.
[10] S.J. Zhang, L. Lebrun, S. Rhee, R.E. Eitel, C.A. Randall, T.R. Shrout, J. Cryst. Growth 236 (2002) 210–216.
[11] S.J. Zhang, D.Y. Jeong, Q.M. Zhang, T.R. Shrout, J. Cryst. Growth 247 (2003) 131–136.
[12] S.J. Zhang, C.A. Randall, T.R. Shrout, Appl. Phys. Lett. 83 (2003) 3150–3152.
[13] S.J. Zhang, S.M. Lee, D.H. Kim, H.Y. Lee, T.R. Shrout, J. Am. Ceram. Soc. 90 (2007) 3859–3862.
[14] Y. Guo, H.S. Luo, T. He, Z. Yin, Solid State Commun. 123 (2002) 417–420.
[15] N. Yasuda, H. Ohwa, D. Hasegawa, K. Hayashi, Y. Hosono, Y. Yamashita, M. Iwata, Y. Ishibashi, Jpn. J. Appl. Phys. 39 (2000) 5586–5588.
[16] Z.Q. Duan, G.S. Xu, X.F. Wang, D.F. Yang, X.M. Pan, P.C. Wang, Sol. State Commun. 134 (2005) 559–563.
[17] J. Tian, P. Han, X. Huang, H. Pan, J.F. Carroll III, D.A. Payne, Appl. Phys. Lett. 91 (2007) 222903.
[18] G.S. Xu, K. Chen, D.F. Yang, J.B. Li, Appl. Phys. Lett. 90 (2007) 032901.
[19] S.J. Zhang, J. Luo, W. Hackenberger, T.R. Shrout, J. Appl. Phys. 104 (2008) 064106.
[20] S.J. Zhang, J. Luo, W. Hackenberger, N.P. Sherlock, R.J. Meyer Jr., T.R. Shrout, J. Appl. Phys. 105 (2009) 104506.
[21] F. Li, S.J. Zhang, Z. Xu, X.Y. Wei, J. Luo, T.R. Shrout, Appl. Phys. Lett. 96 (2010) 192903.
[22] X.Z. Liu, S.J. Zhang, J. Luo, T.R. Shrout, W.W. Cao, J. Appl. Phys. 106 (2009) 074112.
[23] J. Luo, W. Hackenberger, S.J. Zhang, T.R. Shrout, IEEE International Ultrasonics Symposium Proceedings, 2008, pp. 261–264.
[24] IEEE Standards on Piezoelectricity, IEEE, New York, 1987.
[25] N.P. Sherlock, S.J. Zhang, J. Luo, H.Y. Lee, T.R. Shrout, R.J. Meyer Jr., J. Appl. Phys. 107 (2010) 074108.
[26] S.J. Zhang, J. Luo, F. Li, R.J. Meyer Jr., W. Hackenberger, T.R. Shrout, Acta Mater. 58 (2010) 3773–3780.
[27] H.J. Lee, S.J. Zhang, T.R. Shrout, J. Appl. Phys. 107 (2010) 124107.
[28] M. Davis, D. Damjanovic, D. Hayem, N. Setter, J. Appl. Phys. 98 (2005) 014102.
[29] M. Davis, D. Damjanovic, N. Setter, Appl. Phys. Lett. 87 (2005) 102904.
[30] S.J. Zhang, N.P. Sherlock, R.J. Meyer Jr., T.R. Shrout, Appl. Phys. Lett. 94 (2009) 162906.
[31] S.J. Zhang, S.M. Lee, D.H. Kim, H.Y. Lee, T.R. Shrout, Appl. Phys. Lett. 93 (2008) 122908.
[32] H.J. Lee, S.J. Zhang, J. Luo, F. Li, T.R. Shrout, Adv. Funct. Mater. 20 (2010) 3154–3162.
[33] X. Jiang, K. Snook, W. Hackenberger, X. Geng, Proc. SPIE 6531 (2007) 65310F.